# Ⅲ. 研究成果の刊行物・別刷

# CLINICAL CHARACTERISTICS OF OCCULT MACULAR DYSTROPHY IN FAMILY WITH MUTATION OF *RP1L1* GENE

KAZUSHIGE TSUNODA, MD, PHD,* TOMOAKI USUI, MD, PHD,†‡ TETSUHISA HATASE, MD, PHD,† SATOSHI YAMAI, MD,§ KAORU FUJINAMI, MD,* GEN HANAZONO, MD, PHD,* KEI SHINODA, MD, PHD,*¶ HISAO OHDE, MD, PHD,** MASAKAZU AKAHORI, PHD,* TAKESHI IWATA, PHD,* YOZO MIYAKE, MD, PHD*††

**Purpose:** To report the clinical characteristics of occult macular dystrophy (OMD) in members of one family with a mutation of the *RP1L1* gene.

**Methods:** Fourteen members with a p.Arg45Trp mutation in the *RP1L1* gene were examined. The visual acuity, visual fields, fundus photographs, fluorescein angiograms, full-field electroretinograms, multifocal electroretinograms, and optical coherence tomographic images were examined. The clinical symptoms and signs and course of the disease were documented.

**Results:** All the members with the *RP1L1* mutation except one woman had ocular symptoms and signs of OMD. The fundus was normal in all the patients during the entire follow-up period except in one patient with diabetic retinopathy. Optical coherence tomography detected the early morphologic abnormalities both in the photoreceptor inner/outer segment line and cone outer segment tip line. However, the multifocal electroretinograms were more reliable in detecting minimal macular dysfunction at an early stage of OMD.

**Conclusion:** The abnormalities in the multifocal electroretinograms and optical coherence tomography observed in the OMD patients of different durations strongly support the contribution of *RP1L1* mutation to the presence of this disease.

**RETINA** 32:1135–1147, 2012

Occult macular dystrophy (OMD) was first described by Miyake et al[1] to be a hereditary macular dystrophy without visible fundus abnormalities. Patients with OMD are characterized by a progressive decrease of visual acuity with normal-appearing fundus and normal fluorescein angiograms (FA). The important signs of OMD are normal full-field electroretinograms (ERGs) but abnormal focal macular ERGs and multifocal electroretinograms (mfERGs) also exist. These findings indicated that the retinal dysfunction was confined to the macula.[1–5] Optical coherence tomography (OCT) showed structural changes in the outer nuclear and photoreceptor layers.[6–11]

Recently, we found that dominant mutations in the *RP1L1* gene were responsible for OMD.[12] The *RP1L1* gene was originally cloned as a gene derived from common ancestors as a retinitis pigmentosa 1 (*RP1*) gene, which is responsible for 5–10% of autosomal dominant retinitis pigmentosa worldwide, on the same Chromosome 8.[13–17] A number of attempts have been made to identify mutations in *RP1L1* in various retinitis pigmentosa patients with no success. An immunohistochemical study on cynomolgus monkeys showed that *RP1L1* was expressed in rod and cone photoreceptors, and *RP1L1* is thought to play important roles in the morphogenesis of the photoreceptors.[13,18] Heterozygous *RP1L1* knockout mice were reported to be normal, whereas homozygous knockout mice develop subtle retinal degeneration.[18] However, the RP1L1 protein has a very low degree of overall sequence

From the *Laboratory of Visual Physiology, National Institute of Sensory Organs, Tokyo, Japan; †Division of Ophthalmology and Visual Science, Graduate School of Medical and Dental Sciences, Niigata University, Niigata, Japan; ‡Akiba Eye Clinic, Niigata, Japan; §Department of Ophthalmology, Sado General Hospital, Niigata, Japan; ¶Department of Ophthalmology, School of Medicine, Teikyo University, Tokyo, Japan; **Department of Ophthalmology, School of Medicine, Keio University, Tokyo, Japan; and ††Aichi Medical University, Aichi, Japan.

The authors have no financial interest or conflicts of interest.

Supported in part by research grants from the Ministry of Health, Labor and Welfare, Japan and Japan Society for the Promotion of Science, Japan.

Reprint requests: Kazushige Tsunoda, Laboratory of Visual Physiology, National Institute of Sensory Organs, 2-5-1 Higashigaoka, Meguro-ku, Tokyo 152-8902, Japan; e-mail: tsunodakazushige@kankakuki.go.jp

identity (39%) between humans and mice compared with the average values of sequence similarity observed between humans and mice proteins. The results of linkage studies have strongly supported the contribution of *RP1L1* mutations to the presence of this disease,[12] but the function of *RP1L1* in the human retina has not been completely determined.

A large number of cases of OMD have been reported[7,10,19]; however, we did not always find the same mutations in sporadic cases or in small families, which had less than three affected members. This led us to hypothesize that several independent mutations can lead to the phenotype of OMD, that is, OMD is not a single disease caused by a specific gene mutation, but may represent different diseases with similar retinal dysfunctions.

Thus, the aim of this study was to determine the characteristics of OMD by investigating the phenotypes of patients with the *RP1L1* mutation from a single Japanese family.

## Patients and Methods

We investigated 19 members from a single Japanese family. A homozygous mutation, p.Arg45Trp in the *RP1L1* gene, was confirmed in 14 members,[12] and 13 of the 14 were diagnosed with OMD. Among the 14 members with a mutation in the *RP1L1* gene, 11 were followed-up at the Niigata University in Niigata, Japan. The other three were examined at the National Institute of Sensory Organs in Tokyo, Japan. Each member had a complete ophthalmic examination including best-corrected visual acuity (BCVA), refraction, perimetry, fundus photography, FA, full-field ERGs,[20] mfERGs,[21] and OCT. The visual fields were determined by Goldmann perimetry or by Humphrey Visual Field Analyzer (Model 750i; Carl Zeiss Meditec, Inc, Dublin, CA). The SITA Standard strategy was used with the 30-2 program or the 10-2 program for the Humphrey Visual Field Analyzer.

Electroretinograms were used to assess the retinal function under both scotopic and photopic conditions.[22] Full-field ERGs were recorded using the International Society of Clinical Electrophysiology and Vision standard protocol. Multifactorial electroretinograms were recorded with the Visual Evoked Response Imaging System (VERIS science 4.1; EDI, San Mateo, CA). A Burian–Allen bipolar contact lens electrode was used to record the mfERGs. The visual stimuli consisted of 61 or 103 hexagonal elements with an overall subtense of approximately 60°. The luminance of each hexagon was independently modulated between black (3.5 cd/m$^2$) and white (138.0 cd/m$^2$) according to a binary m-sequence at 75 Hz. The surround luminance was 70.8 cd/m$^2$.

The OCT images were obtained with a spectral-domain OCT (HD-OCT; Carl Zeiss Meditec or a 3D-OCT-1000, Mark II; Topcon) from 21 eyes of 12 cases in the same pedigree.

The procedures used adhered to the tenets of the Declaration of Helsinki and were approved by the Medical Ethics Committee of both the Niigata University and National Institute of Sensory Organs. An informed consent was received from all the subjects for the tests.

## Results

The findings of 5 generations of 1 family with OMD are shown in Figure 1. The numbered family members had the same mutation in *RP1L1* (p.Arg45Trp), and family members designated with the filled squares or filled circles were phenotypically diagnosed with OMD by routine examinations including visual field tests, FA, mfERGs, and Fourier-domain OCT. Only Patient 5 (age 60 years) had normal phenotype, although she had the *RP1L1* mutation.

The clinical characteristics and the results of ocular examinations of all the 14 family members with the *RP1L1* mutation (p.Arg45Trp) are listed in Tables 1 and 2. Family Member #5 was diagnosed as normal because she had normal mfERGs.

Among the 13 OMD patients (average age at the final examination, 57.2 ± 22.1 years), 12 complained of disturbances of central vision and 4 complained of photophobia (Table 1). Patient 1 did not report any visual disturbances in the right eye as did Patient 6 for both eyes. The visual dysfunction in these eyes was confirmed by mfERGs. For 13 patients, the age at the onset of visual difficulties varied from 6 years to 50 years with a mean of 27.3 ± 15.1 years.

All the patients were affected in both eyes, and the onset was the same in the 2 eyes except for Patients 1, 11, 12, and 14. Patient 1 first noticed a decrease in her visual acuity in her left eye at age 50 years, and she still did not have any subjective visual disturbances in her right eye 30 years later. However, a clear decrease in the mfERGs in the macular area was detected in both eyes. Patient 11 first noticed a decrease in the visual acuity in her right eye at age 47 years when the BCVA was 0.2 in the right eye and 1.2 in the left eye (Figure 2). Seven years later at age 54 years, she noticed a decrease in the vision in her left eye. Similarly, Patients 12 and 14 did not report any visual disturbances in their right eyes until 2 (Patient 12) or 8 (Patient 14) years after the onset in their left eyes.

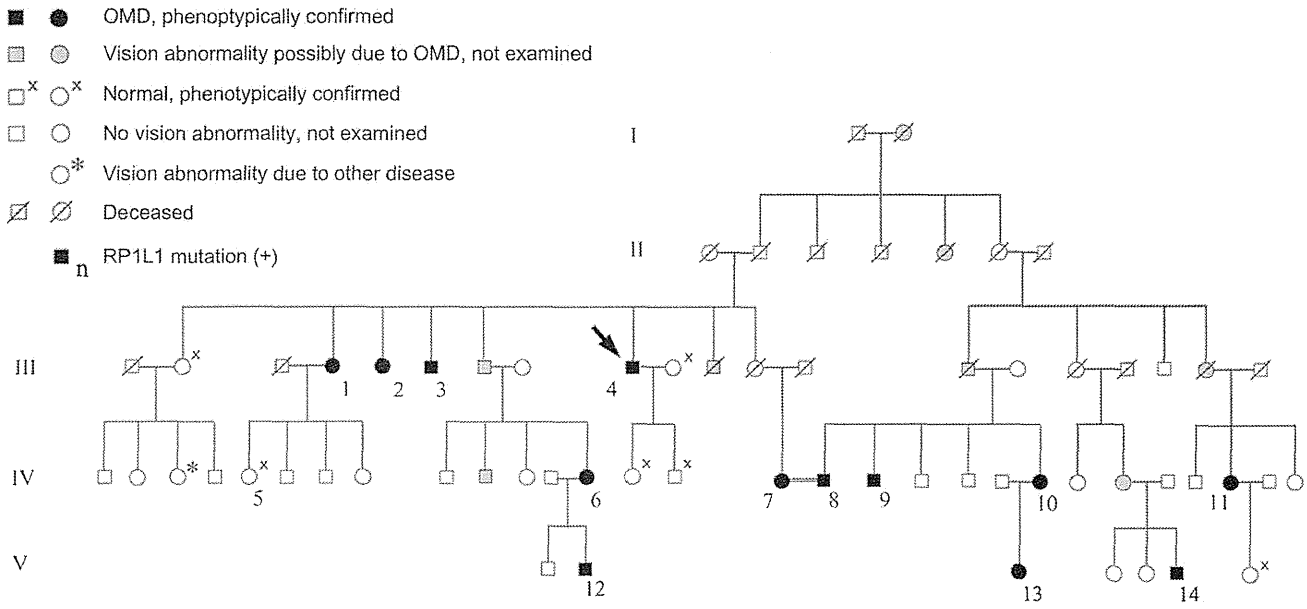


**Fig. 1.** Pedigree of a family with OMD. The identification number of the patients is marked beside the symbols. The proband is indicated by an arrow. The open squares and circles with crosses are the relatives whose visual function was confirmed to be normal by routine examinations including Humphrey visual field tests, mfERGs, and Fourier-domain OCT. Those designated by hatched squares or circles were reported to have poor vision with similar severity and onset as the other genetically confirmed OMD patients. One relative marked by an asterisk had unilateral optic atrophy because of retrobulbar neuritis.

The duration of the continuous decrease in the BCVA varied from 10 years to 30 years (mean, 15.6 ± 7.7 years) in 16 eyes of 9 adult patients. After this period, these patients reported that their vision did not decrease. Patients 2, 3, 8, and 14 complained of photophobia, and the degree of photophobia remained unchanged after the visual acuity stopped decreasing. Patients 1, 2, 4, 7, and 9 had additional disturbances of vision because of senile cataracts, and Patients 2 and 4 had bilateral cataract surgery. The visual disturbances because of the OMD were still progressing at the last examination in the left eye of Patient 11 (age 57 years), and both eyes of Patient 12 (age 20 years), Patient 13 (age 18 years), and Patient 14 (age 28 years).

Different systemic disorders were found in some of the patients; however, there did not seem to be a specific disorder, which was common to all of them (Table 1).

In the 16 eyes of 9 patients whose BCVA had stopped decreasing, the BCVA varied from 0.07 to 0.5 (Table 2). The BCVA of the left eye of Patient 6 was 0.07 because of an untreated senile cataract. If this eye is excluded, the final BCVAs of all the stationary eyes range from 0.1 to 0.5. Patient 2 had photophobia, and her BCVA measured by manually presenting Landolt rings on separate cards under room light was 0.4 in the right eye and 0.5 in the left eye, which was better than that measured by a Landolt chart of 0.3 in the right eye and 0.3 in the left eye with background illumination.

For the 13 patients whose original refractions were confirmed, 11 of 26 eyes were essentially emmetropic ($\leq \pm$ 0.5 diopters). Both eyes of Patients 1, 3, 4, 6, and 8 and the left eye of Patient 5 were hyperopic (+0.675 to +4.625 diopters). The right eye of Patient 7, the left eye of Patient 12, and both eyes of Patient 13 were moderately myopic (−0.625 to −2.75 diopters). These results indicate that there is no specific refraction associated with OMD patients in this family.

The visual fields were determined by Goldmann perimetry or Humphrey Visual Field Analyzer. All the patients had a relative central scotoma in both eyes except for Patient 1 whose right eye was normal by Goldmann perimetry. In all cases, no other visual field abnormalities were detected during the entire course of the disease. In the patients examined shortly after the onset, a relative central scotoma was not detected by Goldman perimetry and was confirmed by static perimetry.

The fundus of all except one eye was normal. The left eye of Patient 9 had background diabetic retinopathy. At the first consultation at age 46 years, Patient 9 did not have diabetes, and the funduscopic examination and FA revealed no macular abnormalities. At the age 66 years, there were few microaneurysms in the left macula away from the fovea; however, OCT did not show any diabetic changes such as macular edema. The OMD was still the main cause of visual acuity reduction in this patient.

Six patients consented to FA, and no abnormality was detected in the entire posterior pole of the eye. It is noteworthy that both the fundus and FA of Patient 4 were normal at the age 73 years, which was >50 years

Table 1. Clinical Characteristics of the Family Members With RP1L1 Mutation (p.Arg45Trp)

| Case | Age and Gender | Chief Complaint | Affected Eye | Age at Onset (Years) | Duration of Continuous Decrease in BCVA (Years) | Duration After the Onset (Years) | Systemic Disorders |
|---|---|---|---|---|---|---|---|
| 1 | 81, F | Decreased visual acuity | Bilateral* | 50 | 20 | 31 | Hypertension |
| 2 | 71, F | Decreased visual acuity and photophobia | Bilateral | 25 | 25 | 46 | Diabetes mellitus since 64 years of age |
| 3 | 74, M | Decreased visual acuity and photophobia | Bilateral | 30 | 10 | 44 | Hyperlipidemia, angina pectoris |
| 4 | 83, M | Decreased visual acuity | Bilateral | 20 | 10 | 63 | Hypertension, Multiple cerebral infarction at 73 years of age |
| 5 | 60, F | None | —† | — | — | — | — |
| 6 | 50, F | None | Bilateral* | Unknown | Unknown | Unknown | — |
| 7 | 69, F | Decreased visual acuity | Bilateral | 50 | 10 | 19 | — |
| 8 | 69, M | Decreased visual acuity and photophobia | Bilateral | 28 | 10 | 41 | Hypertension since 67 years of age, Surgery for ossification of the posterior longitudinal ligament at 45 years of age |
| 9 | 66, M | Decreased visual acuity | Bilateral | 30 | 15 | 36 | Diabetes mellitus since 63 years of age |
| 10 | 58, F | Decreased visual acuity | Bilateral | 10 | 30 | 48 | Rheumatoid arthritis since 46 years of age, Bronchiectasis since 43 years of age |
| 11 | 57, F | Decreased visual acuity | Bilateral ‡ | 47 | OD, 10, OS, still progressing | 10 | — |
| 12 | 20, M | Decreased visual acuity | Bilateral§ | 14 | Still progressing | 6 | Atopic dermatitis |
| 13 | 18, F | Decreased visual acuity | Bilateral | 6 | Still progressing | 12 | — |
| 14 | 28, M | Decreased visual acuity and photophobia | Bilateral¶ | 18 | Still progressing | 10 | — |

*Patient 1 has subjective visual disturbance only in the left eye, and Patient 6 does not have any subjective visual disturbances in both eyes. The visual dysfunction was confirmed by mfERG.

†This woman has a mutation in RP1L1, but her visual function was confirmed normal after routine examinations including mfERG.

‡This patient noticed visual disturbance only in the right eye at 47 years of age. The visual disturbance in the left eye was first noticed at 54 years of age.

§This patient noticed visual disturbance only in the left eye at 14 years of age. The visual disturbance in the right eye was first noticed at 16 years of age.

¶This patient noticed visual disturbance only in the left eye at 18 years of age. The visual disturbance in OD was first noticed at 26 years of age.

Table 2. Results of Ocular Examinations of the Family Members With RP1L1 Mutation

| Case | Age and Gender | BCVA at Final Visit | | Refraction (D)* | | Visual Field | Fundus Appearance | FA | Full-Field ERG | Relative Amplitude in mfERG at Fovea (Ring 1/Ring 5 or Ring 6)† | Other Ocular Disorders |
|---|---|---|---|---|---|---|---|---|---|---|---|
| | | OD | OS | OD | OS | | | | | | |
| 1 | 81, F | 1.2 | 0.1 | +4.25 | +4.625 | Relative central scotoma, OS | Normal, OU | Normal, OU | NE | 2.34, OD, 0.60, OS | Senile cataract, OU |
| 2 | 71, F | 0.4 | 0.5 | Unknown‡ | Unknown‡ | Relative central scotoma, OU | Normal, OU | NE | NE | Not measurable, OU | Cataract surgery, OS at 58 years of age, OD at 69 years of age, Ptosis, OU |
| 3 | 74, M | 0.2 | 0.3 | +2.875 | +3.375 | Relative central scotoma, OU | Normal, OU | NE | NE | Not measurable, OU | Laser peripheral iridotomy, OU at 73 years of age |
| 4 | 83, M | 0.2 | 0.2 | +1.0 | +1.625 | Relative central scotoma, OU | Normal, OU | Normal, OU | Normal ISCEV standard protocol ERG, OU | Not measurable, OU | Cataract surgery, OU at 80 years of age |
| 5 | 60, F | 1.2 | 1.2 | −0.25 | +0.875 | Normal, OU | Normal, OU | NE | NE | 4.24, OD, NE, OS | — |
| 6 | 50, F | 1.2 | 1.2 | +1.0 | +1.0 | Relative central scotoma, OU | Normal, OU | NE | NE | 2.74, OD, 2.23, OS | — |
| 7 | 69, F | 0.1§ | 0.07§ | −0.625 | +0.25 | Relative central scotoma, OU | Normal, OU | NE | Normal ISCEV standard protocol ERG, OU | Not measurable, OU | Senile cataract, OU |
| 8 | 69, M | 0.1 | 0.1 | +1.125 | +0.675 | Relative central scotoma, OU | Normal, OU | NE | Normal ISCEV standard protocol ERG, OU | 1.01, OD, 1.30, OS | — |

Table 2. (Continued)

| Case | Age and Gender | BCVA at Final Visit | | Refraction (D)* | | Visual Field | Fundus Appearance | FA | Full-Field ERG | Relative Amplitude in mfERG at Fovea (Ring 1/Ring 5 or Ring 6)† | Other Ocular Disorders |
|---|---|---|---|---|---|---|---|---|---|---|---|
| | | OD | OS | OD | OS | | | | | | |
| 9 | 66, M | 0.2 | 0.3 | +0.125 | +0.125 | Relative central scotoma, OU | Normal, OD Background diabetic retinopathy with microaneurysm, OS | Normal, OU | Normal mixed rod–cone responses, OU | 1.21, OD1.59, OS | Senile cataract, OU |
| 10 | 58, F | 0.1 | 0.1 | +0.5 | +0.375 | Relative central scotoma, OU | Normal, OU | NE | Normal cone responses, OU | Not measurable, OU | — |
| 11 | 57, F | 0.1 | 0.4 | +0.5 | 0.0 | Relative central scotoma, OU | Normal, OU | Normal, OU | Normal ISCEV standard protocol ERG, OU | Not measurable, OU | — |
| 12 | 20, M | 0.3 | 0.3 | −0.375 | −0.75 | Relative central scotoma, OU | Normal, OU | Normal, OU | Normal ISCEV standard protocol ERG, OU | 0.98, OD1.03, OS | — |
| 13 | 18, F | 0.2 | 0.15 | −1.625¶ | −2.75¶ | Relative central scotoma, OU | Normal, OU | Normal, OU | Normal ISCEV standard protocol ERG, OU | Not measurable, OU | — |
| 14 | 28, M | 1.0 | 0.6 | −0.25 | −0.25 | Relative central scotoma, OU | Normal, OU | NE | Normal ISCEV standard protocol ERG, OU | 1.63, OD, 0.66, OS | — |

D, diopter; ISCEV, International Society of Clinical Electrophysiology and Vision; NE, not examined.
*Spherical equivalents at the initial visit.
†The responses of Ring 1 were extinguished and the N1–P1 amplitudes were not measurable in Cases 2, 3, 4, 7, 10, 11, and 13.
‡This patient had already undergone cataract surgeries for both eyes at the initial visit, and no data could be obtained about the original refraction.
§This patient's visual acuity was reduced also by senile cataract.
¶The refraction of this patient was measured after instillation of cycloplegics.

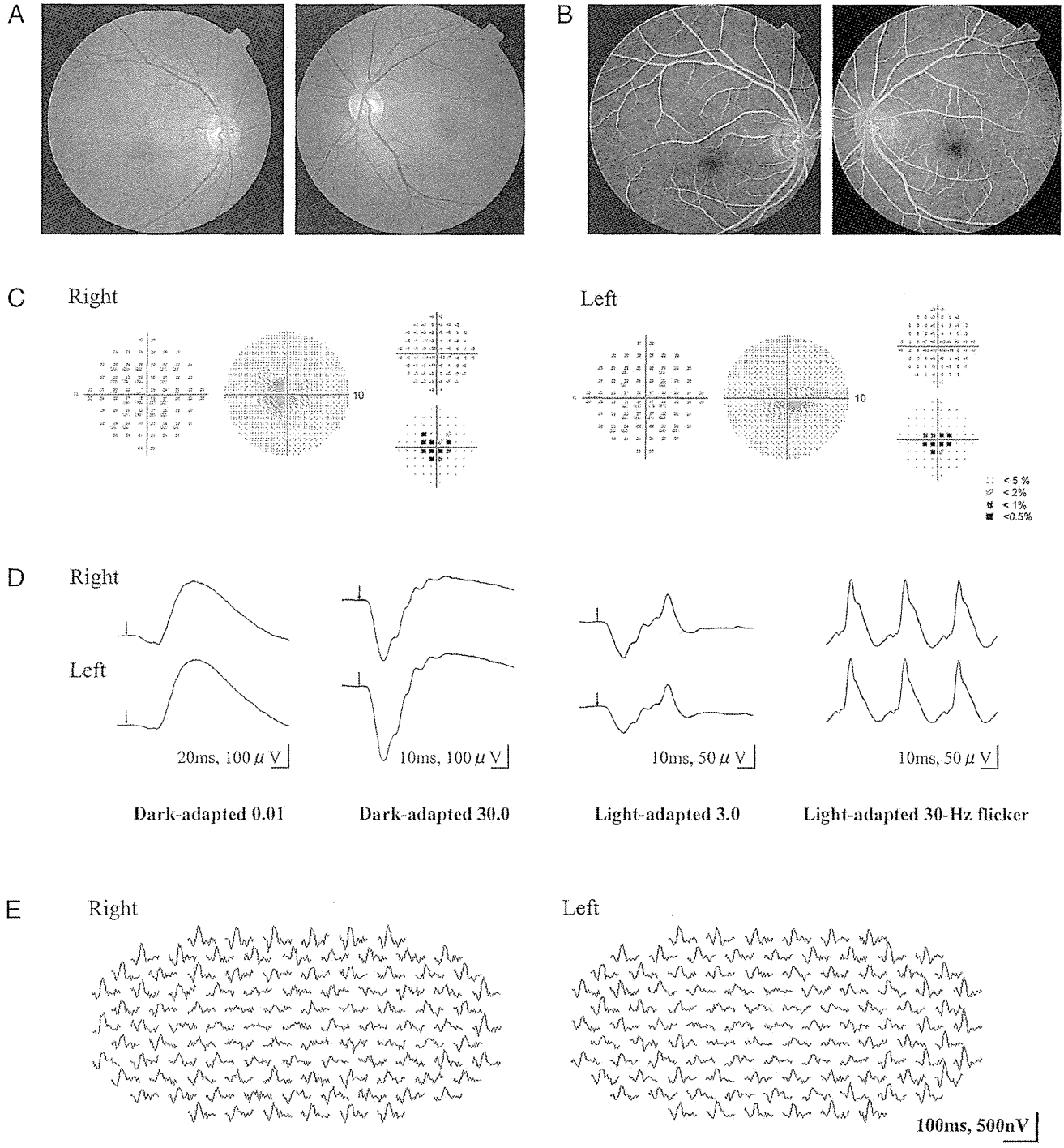


**Fig. 2.** Results of ocular examination of Patient 11. The data in (**A**) to (**E**) were collected 3 years after the onset of the visual disturbance at age 50 years. At this time, the patient had not noticed a decrease in the visual acuity in her left eye. The BCVA was 0.1 in the right eye and 1.2 in the right eye. **A**, and **B**. Fundus photographs and FAs showing no abnormal findings. **C**. Static visual field test (Humphrey Visual Field Analyzer, 10-2) showing relative central scotoma in both eyes. **D**. Full-field rod, mixed rod–cone, cone ERGs, and 30-Hz flicker responses. All the responses are normal in both eyes. **E**. Trace arrays of mfERGs tested with 103 hexagonal stimuli shown without spatial averaging. The responses of the central locus are extinguished in both eyes.

after the onset. This patient first noticed visual disturbances at age 20 years and was diagnosed with OMD at age 73 years. The appearance of the macula and optic disk at age 83 years was still normal >60 years after the onset of the symptoms.

Rod, mixed rod–cone, and cone full-field ERGs were recorded from 7 patients using the International Society of Clinical Electrophysiology and Vision standard protocol, and all of them showed normal rod and cone responses as in the representative case shown in

Figure 2. Only the mixed rod–cone responses were recorded from Patient 9, and only the cone responses were recorded from Patient 10, and these responses were also normal.

The amplitudes of the mfERGs were reduced in the central region of both eyes in all the 13 patients. We quantified the relative mfERG responses at the fovea by dividing the N1–P1 amplitudes of the central ring (Ring 1) by those in the outermost eccentric ring (Ring 5 in cases of 61 stimuli and Ring 6 in cases of 103 stimuli) in 13 OMD patients and 1 normal family member (Case 5) with the *RP1L1* mutation (Table 2).[4] Among the 26 eyes of the 13 OMD patients, the N1–P1 amplitudes of the central locus were measurable in 12 eyes in 6 cases tested with the 61 stimuli. The ratio of the amplitudes of Ring 1/Ring 5 in these OMD patients ranged from 0.60 to 2.74 (average of normals: 4.34 ± 0.67, n = 20). In 6 eyes tested with 61 stimuli and all the 8 eyes tested with 103 stimuli, the responses in the central locus were extinguished and the amplitudes were not measurable (see examples in Figure 2E). The ratio of the amplitudes of Ring 1/Ring 5 in a normal family member (Case 5, right eye) was 4.24, which was within the normal range.

The results of routine ocular examinations in Patient 11 at the age 50 years, when she did not have any visual disturbances in her left eye, are shown in Figure 2. The BCVA was 0.1 in the right eye and 1.2 in the left eye. The fundus and FA were normal in both eyes. Humphrey visual field tests (SITA Standard and pattern deviation 10-2) showed a relative central scotoma in both eyes. The full-field rod, mixed rod–cone, cone, and 30-Hz flicker ERGs were normal in both eyes. The mfERGs were reduced in and around the region of the central scotoma in both eyes. The Humphrey visual field test (30-2) did not detect a central scotoma in either eye (data not shown). The findings in the left eye of this patient are typical of the early stage of the OMD, where the dysfunction of the foveal region could be clearly detected in the mfERGs even though the subjective visual disturbance was almost undetectable.

Spectral-domain OCT images were recorded from 11 family members with the *RP1L1* mutation. The outer retinal structure was considered to be normal when the external limiting membrane, photoreceptor inner/outer segment (IS/OS) line, cone outer segment tip (COST) line, and retinal pigment epithelium (RPE) were clearly detected in the OCT images (Figure 3A).[11,23]

The OCT images of 5 representative OMD patients are aligned in the order of years after the onset in Figure 3B. The right eye of Case 1, which had electrophysiologically confirmed macular dysfunction but did not have subjective visual disturbances, showed a normal IS/OS line and COST line but only at the foveal center (asterisk in Figure 3B, ①). However, in the parafoveal region, the IS/OS line was blurred and the COST line could not be observed (arrowheads in Figure 3B, ①).

In the right eye of Case 11, the OCT images which were taken 10 years after the onset showed that the IS/OS line at the fovea was very blurred and thick but not disrupted. The COST line could not be observed in the macular area. In the perimacular region that had normal visual function, all the outer retinal structures were seen to be normal (Figure 3B, ②). Similar findings were observed in the left eye of Case 1 and the right eye of Case 8 (Figure 3B, ③ and ④).

In the right eye of Case 4, which was examined 63 years after the onset, the IS/OS line was disrupted at the fovea. The COST line could not be observed in the macula but was still visible in the perimacular region. The external limiting membrane and RPE could be observed to be normal over the entire region (Figure 3B, ⑤).

The OCT images of 2 sporadic cases of OMD without the *RP1L1* mutation are shown in Figure 3C. Both patients had a progressive central scotoma with normal-appearing fundus and normal FA. The full-field ERGs were normal but the focal macular ERGs elicited with a 10° spot were not recordable. Their OCT images, however, were not similar to those in patients with *RP1L1* mutation; the IS/OS line could be clearly observed at the fovea (Figure 3C, ①and ②), and the COST line could also be observed at the fovea, although it was slightly more blurred than in the normal cases. There was a minute disruption of the IS/OS line at the foveola in 1 case (asterisk in Figure 3C, ①).

The OCT findings in 21 eyes of 11 cases with the *RP1L1* mutation are summarized in Table 3. The examined eyes are listed in the order of years after the onset. Case 5, who was diagnosed as not having the typical characteristics of OMD, had completely normal retinal structures. In the case of OMD without subjective visual disturbances, the COST line and IS/OS line were normally observed only at the very center of the fovea (Case 1, right eye, Figure 3B, ①). In other affected cases, the COST line was not present and the IS/OS line appeared blurred in the entire fovea (Cases 14, right eye to 8). In patients with longer duration OMD, the IS/OS line was disrupted or not present as in Cases 2 and 4.

The retinal thickness at the foveola was measured as the distance from the internal limiting membrane to the inner border of the RPE. Considering the variation in the thickness in normals, we classified that the retina at the foveola was abnormally thin when the thickness was $<160$ $\mu$m. All the affected eyes with disease duration $\leq 12$ years had normal foveal thickness (right

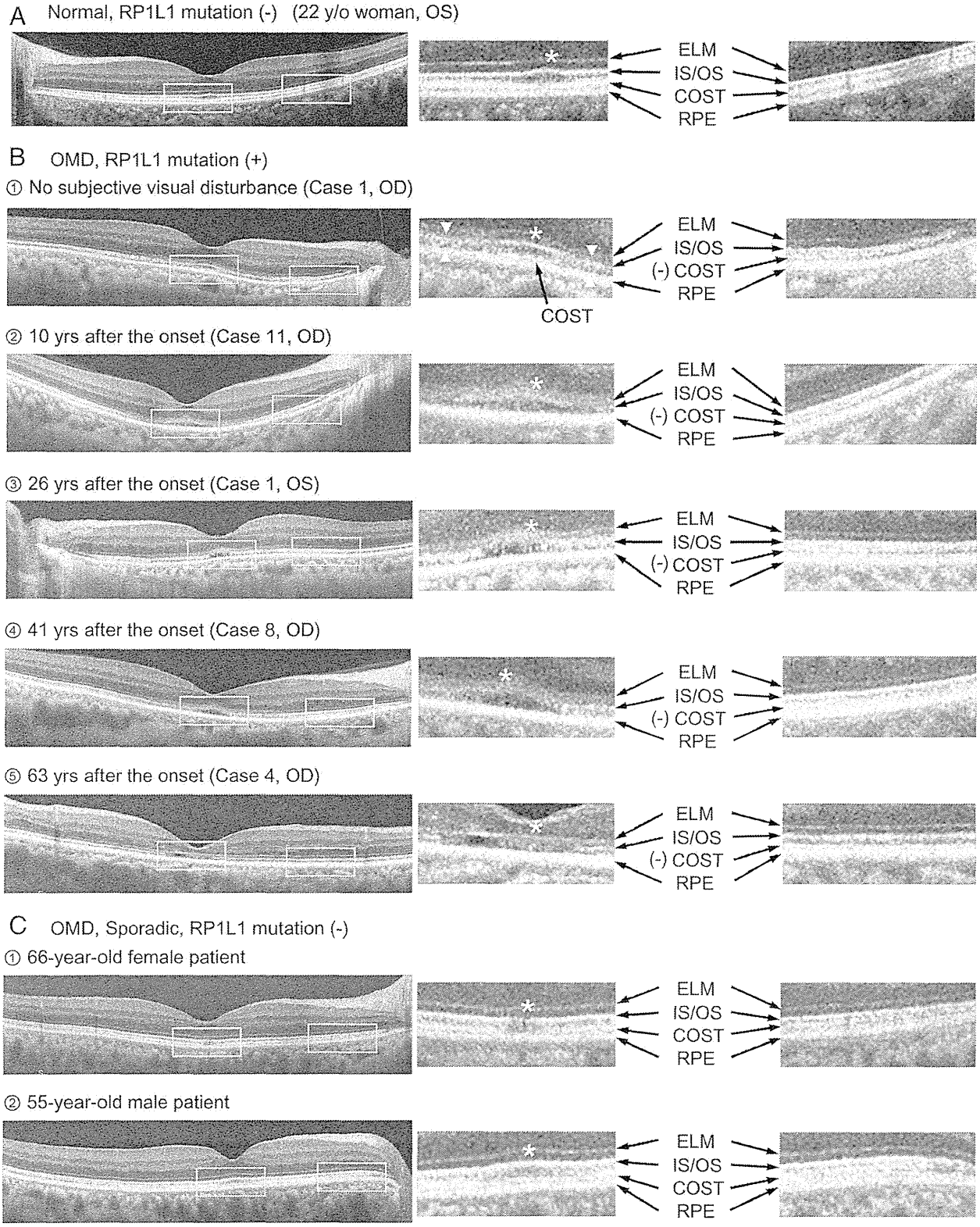


**Fig. 3.** Optical coherence tomography images horizontally profiled along the foveola (left) and magnified images in the fovea and the perimacular region (right). Outer retinal structures, such as external limiting membrane (ELM), photoreceptor IS/OS line, COST line, and RPE, are indicated by arrows. The foveal center is indicated by an asterisk. All the OCT images were taken with the HD-OCT (Carl Zeiss). **A.** Optical coherence tomography image of a normal control without the *RP1L1* mutation (22-year-old woman). All the outer retinal structures, for example, external limiting membrane, IS/OS line, COST line, and RPE, are clearly observed both in the fovea and the perimacular region. **B.** Optical coherence tomography images of patients affected by OMD with the *RP1L1* mutation. ①. Optical coherence tomography image of the right eye of Case 1, which did not have subjective visual disturbances. The COST line is present in the foveal center (black arrow), but not in the parafoveal region (arrowheads). The IS/OS line is clearly

eye of Cases 1 to Case13), whereas the fovea of all the affected eyes with durations ≥20 years were classified as thin (Case 7 to Case 4).

To determine whether a significant correlation existed between the results of mfERGs and OCT, the relative amplitudes of the mfERGs at the fovea (Ring 1/Ring 5 or 6) are listed in Table 3. In cases where the disease durations was ≥3 years, the relative amplitude at the fovea was approximately 1.0 or nonrecordable because the responses of the central locus were extinguished. Only cases with very short durations had mildly reduced mfERGs in the fovea (2.34 in the right eye of Case 1 and 1.63 in the right eye of Case 14).

## Discussion

### *Course of OMD Patients with RP1L1 Mutation*

Our results confirmed that all the patients with the *RP1L1* mutation had similar phenotypes; slowly progressive visual disturbances of both eyes, normal-appearing fundus, normal FA and full-field ERGs during the entire course of the disease, selective dysfunction at the macula detected by focal macular ERGs and mfERGs, selective abnormality of the photoreceptor layer in the macula revealed by OCT, and a final BCVA not poorer than 0.1. The age at the onset of OMD was, however, very variable among the family members and varied from 6 years to 50 years.

Our study also confirmed that there are patients with OMD who have normal visual acuity and no subjective visual disturbances until the disease progressed to a more advanced stage. Similar findings have been reported for other patients with OMD,[1,2,24] although the etiology of these patients was not confirmed by genetic analyses. For such patients, the function of the small region in the foveola of these eyes has probably been spared so that the BCVA was normal. This was morphologically confirmed by the OCT; in the right eye of Case 1, the BCVA of which was 1.2, the OCT image showed that photoreceptor structures were spared only at the foveal center.

Among the 14 family members with the *RP1L1* mutation, only Case 5 (60-year-old woman) did not show any signs of macular dysfunction in both subjective and objective tests. Thus, this woman may be a carrier of a mutated gene, but we cannot exclude the possibility that macular dysfunction may appear later. In our genetic study of 4 other OMD families, 2 brothers (58 and 55 years old) were not diagnosed with OMD, although both had the *RP1L1* mutation (p.Arg45Trp).[12] In all the OMD patients with the *RP1L1* mutation, the visual dysfunction was detected no later than 50 years of age.[12]

Occult macular dystrophy has been reported to be a slowly progressive disease; however, there were no patients whose BCVA became worse than 0.1 except for Patient 7 who had an untreated senile cataract. Our results confirmed that once the BCVA is reduced to 0.1 to 0.2, the disease becomes stationary and both the subjective and objective visual functions do not deteriorate thereafter. Similarly, in 3 other families with the *RP1L1* mutation, the final BCVA was not worse than 0.15 in any member.[12]

There was 1 family member (asterisk, Figure 1) who had a sudden decrease of vision in the left eye at age 49 years, but she was diagnosed with retrobulbar neuritis at the Niigata University. Her vision did not recover after steroid pulse therapy, and the optic disk gradually became atrophic. The BCVA 1 year later was 1.2 in the right eye and 0.07 in the left eye. We concluded that the vision reduction was not related to the OMD. Nakamura et al[25] reported a case of OMD that had normal-tension glaucoma with abnormal cupping of the optic disk. To date, the relationship between OMD and optic disk diseases has not been determined. In our family, the optic disks of all the OMD patients appeared normal, and OCT did not show any thinning of the nerve fiber layer or ganglion cell layer in any of the patients.

### *Diagnostic Reliabilities of mfERGs and OCT*

There were patients, such as Case 6 (both eyes), Case 1 (right eye), and Case 11 (left eye), with OMD from an *RP1L1* mutation who did not have any subjective visual disturbances and whose diagnosis were only confirmed by the electrophysiologic tests. These

**Figure 3. (continued)** observed at the foveal center (asterisk) but appears blurred in the parafoveal region (arrowheads). ②, ③, and④. Optical coherence tomography image of the right eye of Case 11, the left eye of Case 1, and the right eye of Case 8, which show typical signs of OMD. The COST line is not present over the entire macula but is present in the perimacular regions. The IS/OS line is blurred and thick in the fovea. ⑤. Optical coherence tomography image (vertical section) of the right eye of Case 4. This image was obtained 63 years after the onset of visual symptoms. The IS/OS line is disrupted at the fovea. The COST line cannot be seen in the macula but is still visible in the perimacular region. There is an apparent thinning of the photoreceptor layer at the fovea. **C**. Optical coherence tomography images of sporadic cases of OMD without the *RP1L1* mutation. ① and ②. Both patients had progressive central scotoma with normal-appearing fundus and normal FA. The full-field ERGs were normal but focal macular ERGs elicited by a 10° spot were not recordable. The IS/OS line could be clearly observed at the fovea in both cases, except in minute disruption at the foveola in ① (asterisk). The COST line could be observed at the fovea in both cases, although slightly more blurred than in the normal case.

Table 3. Optical Coherence Tomography Findings in 21 Eyes of 11 Family Members with RP1L1 Mutation in the Order of Years After the Onset

| Years After the Onset (Years) | Case | OD/ OS | BCVA | Relative Amplitude in mfERG at fovea (Ring 1/Ring 5 or 6) | OCT Findings at Fovea: Disappearance of COST at fovea | OCT Findings at Fovea: Blurring of IS/OS Junction at Fovea | OCT Findings at Fovea: Abnormality of RPE | OCT Findings at Fovea: Thinning of Fovea (Thickness <160 μm) | Other Findings |
|---|---|---|---|---|---|---|---|---|---|
| None | 5 | OD | 1.2 | 4.24 | – | – | – | –(217) | Not diagnosed as OMD |
| Unknown | 1 | OD | 1.2 | 2.34 | ±* | ±* | – | –(200) | No subjective visual disturbance |
| 2 | 14 | OD | 1.0 | 1.63 | + | + | – | –(160) | |
| 3 | 11 | OS | 0.4 | Not measurable | + | + | – | –(168) | |
| 6 | 12 | OD | 0.3 | 0.98 | + | + | – | –(174) | |
| | | OS | 0.3 | 1.03 | + | + | – | –(168) | |
| 10 | 14 | OS | 0.6 | 0.66 | + | + | – | –(160) | |
| 10 | 11 | OD | 0.1 | Not measurable | + | + | – | –(164) | |
| 12 | 13 | OD | 0.2 | Not measurable | + | + | – | –(181) | |
| | | OS | 0.15 | Not measurable | + | + | – | –(177) | |
| 20 | 7 | OD | 0.1 | Not measurable | + | + | – | +(134) | |
| | | OS | 0.07 | Not measurable | + | + | – | +(142) | |
| 31 | 1 | OS | 0.1 | 0.60 | + | + | – | +(150) | |
| 38 | 10 | OD | 0.1 | Not measurable | + | + | – | +(150) | |
| | | OS | 0.1 | Not measurable | + | + | – | +(153) | |
| 41 | 8 | OD | 0.1 | 1.01 | + | + | – | +(148) | |
| | | OS | 0.1 | 1.30 | + | + | – | +(148) | |
| 46 | 2 | OD | 0.4 | Not measurable | + | +† | – | +(156) | |
| | | OS | 0.5 | Not measurable | + | +† | – | +(154) | |
| 63 | 4 | OD | 0.2 | Not measurable | + | +† | – | +(77) | |
| | | OS | 0.2 | Not measurable | + | +† | – | +(76) | |

*The COST and IS/OS junction were normal only at the foveal center. In the parafovea, the COST could not be observed and the IS/OS junction was blurred.
†The IS/OS junction was disrupted at the fovea.

findings indicate that mfERGs or focal macular ERGs are sensitive enough to detect very early macular dysfunction in OMD.

Similarly, OCT could be another sensitive tool for the detection of early OMD because an abnormality of the COST line and the IO/OS line in the macula was observed in all the affected cases. However, we believe that the mfERG is more sensitive than OCT in detecting early dysfunctions of the macula in eyes with OMD. For example, Case 14 was a 28-year-old man whose BCVA was 1.0 (right eye) and 0.6 (left eye), but his fundus and visual field tests did not show any differences between the 2 eyes. He did notice a visual disturbance in his left eye 8 years before the onset in his right eye. In the OCT images, both the COST line and the IS/OS line were similarly affected for both eyes at the fovea, and the retinal thickness at the fovea was 160 $\mu$m in both eyes (Table 3). The mfERGs, on the other hand, were different in the 2 eyes; the relative amplitude of mfERG at the fovea (Ring 1/Ring 5) was 1.63 (38.2/23.5) in his right eye and 0.66 (15.8/23.8) in his left eye (Table 3). Thus, we believe that both the mfERGs and OCT can be useful in the diagnosis of OMD, but mfERGs are more reliable in detecting and evaluating minimal macular dysfunction at the early stage of the disease. The abnormalities in the OCT, however, progress slowly and continuously until the late stage, and thus they may be more useful for following the long-term progression of OMD.

*Roles of RP1L1* Gene and Occurrence of OMD

Our study confirmed that all the affected patients with *RP1L1* mutation had abnormalities of the photoreceptor structures; the IS/OS line was very blurred and thick and the COST line could not be observed in the macula (Figure 2). But in the perimacular region, which had normal visual function, all the outer retinal structures were seen to be normal. During the whole disease process, neither the external limiting membrane nor the RPE had any significant changes and remained normal. In some of sporadic cases of the OMD, similar abnormalities in the OCT could not be observed, although localized macular dysfunction was confirmed electrophysiologically (Figure 3C).

The location of COST line coincided with the location where the outer segment disks are renewed in the cones.[23,26] The disappearance of the COST line indicates an early stage of dysfunction of the cone photoreceptors as has been found in acute zonal occult outer retinopathy.[11] Recently, ultrahigh-resolution OCT with adaptive optics has revealed that the IS/OS line corresponds to the ellipsoids of the photoreceptor inner segments, which are rich in mitochondria and play important roles in cellular metabolism.[27]

Immunohistochemistry for the *RP1L1* gene in retinal section of cynomolgus monkeys showed that it was expressed in both the inner and outer segments of the rod and cone photoreceptors, although the exact site within the photoreceptor has not been confirmed.[12] *RP1L1* is believed to play important roles in the morphogenesis of photoreceptors, and once the function of *RP1L1* is disrupted by a mutation, both the electrophysiologic responses and structures of the photoreceptor can be altered. Cellular dysfunction because of an *RP1L1* mutation affects either the inner or outer segment, or both, of the photoreceptors, which first becomes apparent as an abnormality of both the COST line and IS/OS line in the OCT images.

Considering that the OCT abnormalities in sporadic cases did not show similar pattern as patients with the *RP1L1* mutation, the phenotypically confirmed OMD surely consists of diseases caused by several independent etiologies. In any case, the abnormalities in the mfERGs and OCT observed in OMD in this family strongly support the contribution of *RP1L1* mutation to the presence of this disease.

There are still some important questions of the disease process in OMD that are unsolved. First, why is only the macular region affected while the perimacular region remains intact both functionally and morphologically even at a very advanced stage? Second, why do OMD patients have normal fundus appearance until the end stage, and why does the RPE remain intact until the end stage when the photoreceptor structures are markedly damaged (Figure 3B, ⑤)? Fujinami et al[28] demonstrated that the fundus autofluorescence images in the macula of OMD patients are normal, indicating that the RPE is normal. Third, why does the disease progression stop when the BCVA decreases to 0.1 to 0.2?

These characteristics in the disease process are peculiar to the OMD and not observed in other macular dystrophies. More detailed investigations on the function of *RP1L1* should provide information to answer these questions.

We suggest that OMD is not a single disease caused by a specific gene mutation, *RP1L1*, but may represent different disease entities with similar retinal dysfunctions. Considering all our findings on OMD, we can phenotypically define the OMD as a slowly progressing bilateral dysfunction of the photoreceptors located in the macula, not accompanied by either vascular or RPE damage. The etiology of OMD cases without the *RP1L1* mutation is now under investigation with large number of cases and some of them might be found to be because of other autosomal recessive mutations.

**Key words:** electroretinography, focal macular ERG, multifocal ERG, occult macular dystrophy, optical coherence tomography, *RP1L1*.

## References


1. Miyake Y, Ichikawa K, Shiose Y, Kawase Y. Hereditary macular dystrophy without visible fundus abnormality. Am J Ophthalmol 1989;108:292–299.
2. Miyake Y, Horiguchi M, Tomita N, et al. Occult macular dystrophy. Am J Ophthalmol 1996;122:644–653.
3. Fujii S, Escano MF, Ishibashi K, et al. Multifocal electroretinography in patients with occult macular dystrophy. Br J Ophthalmol 1999;83:879–880.
4. Piao CH, Kondo M, Tanikawa A, et al. Multifocal electroretinogram in occult macular dystrophy. Invest Ophthalmol Vis Sci 2000;41:513–517.
5. Wildberger H, Niemeyer G, Junghardt A. Multifocal electroretinogram (mfERG) in a family with occult macular dystrophy (OMD). Klin Monatsbl Augenheilkd 2003;220:111–115.
6. Kondo M, Ito Y, Ueno S, et al. Foveal thickness in occult macular dystrophy. Am J Ophthalmol 2003;135:725–728.
7. Brockhurst RJ, Sandberg MA. Optical coherence tomography findings in occult macular dystrophy. Am J Ophthalmol 2007; 143:516–518.
8. Koizumi H, Maguire JI, Spaide RF. Spectral domain optical coherence tomographic findings of occult macular dystrophy. Ophthalmic Surg Lasers Imaging 2009;40:174–176.
9. Lubinski W, Goslawski W, Penkala K, et al. A 43-year-old man with reduced visual acuity and normal fundus: occult macular dystrophy—case report. Doc Ophthalmol 2008;116:111–118.
10. Park SJ, Woo SJ, Park KH, et al. Morphologic photoreceptor abnormality in occult macular dystrophy on spectral-domain optical coherence tomography. Invest Ophthalmol Vis Sci 2010;51:3673–3679.
11. Tsunoda K, Fujinami K, Miyake Y. Selective abnormality of cone outer segment tip line in acute zonal occult outer retinopathy as observed by Spectral domain optical coherence tomography. Arch Ophthalmol 2011;129:1099–1101.
12. Akahori M, Tsunoda K, Miyake Y, et al. Dominant mutations in RP1L1 are responsible for occult macular dystrophy. Am J Hum Genet 2010;87:424–429.
13. Conte I, Lestingi M, den Hollander A, et al. Identification and characterisation of the retinitis pigmentosa 1-like1 gene (RP1L1): a novel candidate for retinal degenerations. Eur J Hum Genet 2003;11:155–162.
14. Bowne SJ, Daiger SP, Malone KA, et al. Characterization of RP1L1, a highly polymorphic paralog of the retinitis pigmentosa 1 (RP1) gene. Mol Vis 2003;9:129–137.
15. Pierce EA, Quinn T, Meehan T, et al. Mutations in a gene encoding a new oxygen-regulated photoreceptor protein cause dominant retinitis pigmentosa. Nat Genet 1999;22: 248–254.
16. Sullivan LS, Heckenlively JR, Bowne SJ, et al. Mutations in a novel retina-specific gene cause autosomal dominant retinitis pigmentosa. Nat Genet 1999;22:255–259.
17. Jacobson SG, Cideciyan AV, Iannaccone A, et al. Disease expression of RP1 mutations causing autosomal dominant retinitis pigmentosa. Invest Ophthalmol Vis Sci 2000;41: 1898–1908.
18. Yamashita T, Liu J, Gao J, et al. Essential and synergistic roles of RP1 and RP1L1 in rod photoreceptor axoneme and retinitis pigmentosa. J Neurosci 2009;29:9748–9760.
19. Lyons JS. Non-familial occult macular dystrophy. Doc Ophthalmol 2005;111:49–56.
20. Marmor MF, Fulton AB, Holder GE, et al. ISCEV Standard for full-field clinical electroretinography (2008 update). Documenta Ophthalmologica 2009;118:69–77.
21. Hood DC, Bach M, Brigell M, et al. ISCEV guidelines for clinical multifocal electroretinography (2007 edition). Documenta Ophthalmologica 2008;116:1–11.
22. Usui T, Tanimoto N, Ueki S, et al. ERG rod a-wave in Oguchi disease. Vision Research 2004;44:535–540.
23. Srinivasan VJ, Monson BK, Wojtkowski M, et al. Characterization of outer retinal morphology with high-speed, ultrahigh-resolution optical coherence tomography. Invest Ophthalmol Vis Sci 2008;49:1571–1579.
24. Miyake Y. Electrodiagnosis of Retinal Diseases. Tokyo, Japan: Springer-Verlag; 2006.
25. Nakamura M, Kanamori A, Seya R, et al. A case of occult macular dystrophy accompanying normal-tension glaucoma. Am J Ophthalmol 2003;135:715–717.
26. Anderson DH, Fisher SK, Steinberg RH. Mammalian cones–disk shedding, phagocytosis, and renewal. Invest Ophthalmol Vis Sci 1978;17:117–133.
27. Fernandez EJ, Hermann B, Povazay B, et al. Ultrahigh resolution optical coherence tomography and pancorrection for cellular imaging of the living human retina. Opt Express 2008;16: 11083–11094.
28. Fujinami K, Tsunoda K, Hanazono G, et al. Fundus autofluorescence in autosomal dominant occult macular dystrophy. Arch Ophthalmol 2011;129:579–602.

# Outer Retinal Morphology and Visual Function in Patients With Idiopathic Epiretinal Membrane

*Ken Watanabe, MD; Kazushige Tsunoda, MD, PhD; Yoshinobu Mizuno, MD; Kunihiko Akiyama, MD; Toru Noda, MD*

**Objective:** To determine the relationship between the morphology of the fovea and visual acuity in patients with an untreated idiopathic epiretinal membrane (ERM).

**Methods:** We examined 52 eyes of 45 patients diagnosed with an ERM. The morphology of the foveal area was determined by spectral-domain optical coherence tomography. The relationships between the best-corrected visual acuity (BCVA) and 8 optical coherence tomography features, central retinal thickness, cone outer segment tip (COST) line, photoreceptor inner/outer segment (IS/OS) junction line, foveal bulge of the IS/OS line, external limiting membrane, inner limiting membrane, foveal pit, and ERM over the foveal center, were evaluated.

**Results:** Multiple regression analysis showed that intact COST line, IS/OS junction line, and external limiting membrane independently and significantly contributed to the BCVA. The standardized partial regression coefficient β was 0.415 for the COST line, 0.287 for the IS/OS junction line, and 0.247 for the external limiting membrane. However, the other features, eg, foveal bulge, inner limiting membrane, foveal pit, and ERM, were not significantly associated with the BCVA. The central retinal thickness was significantly correlated with the BCVA ($r^2$=0.274; $P<.01$).

**Conclusions:** At an early stage of an ERM, only the photoreceptor structures are significantly associated with the BCVA, and the appearance of the COST line was most highly associated. Detailed examinations of the photoreceptor structures using optical coherence tomography may help find photoreceptor dysfunction in cases of idiopathic ERM.

*JAMA Ophthalmol. 2013;131(2):172-177*

OPTICAL COHERENCE TOmography (OCT) is a useful method of detecting early morphological changes in retinas affected by various pathological conditions. The correlations between the visual acuity and the morphological changes in the retina have been reported for various retinal diseases, such as age-related macular degeneration,[1] central serous chorioretinopathy,[2] macular edema,[3,4] idiopathic macular hole,[5,6] and epiretinal membrane (ERM).[7-9]

Retinal traction caused by an ERM leads to morphological changes of not only the superficial layers of the retina but also the entire retina including the photoreceptor layer. This is important because long-standing morphological changes can lead to functional damages and cause metamorphopsia and decreased visual acuity.

Spectral-domain OCT (SD-OCT) has enabled clinicians and investigators to obtain clearer images of the microstructure of the photoreceptor layer than time-domain OCT. Several studies have examined whether significant correlations exist between macular dysfunction and the integrity of photoreceptor microstructures, especially the photoreceptor inner segment/outer segment (IS/OS) junction line, detected by SD-OCT in patients with an ERM.[7-10]

The diagnostic value of determining the integrity of the IS/OS junction line and the cone outer segment tip (COST) line by SD-OCT has been done primarily on diseases of the outer retina, eg, acute zonal occult outer retinopathy[11] and hereditary macular dystrophies.[12-14] However, in eyes with an ERM, the appearance of the photoreceptor microstructures in the SD-OCT image can be affected by retinal thickening, subretinal cysts, and the ERM itself. These alterations lead to a reduction in the intensity of the laser light reaching the photoreceptor layer. In addition, the clarity of the SD-OCT images of the outer retina, eg, the Henle layer, IS/OS junction line, and COST line, is dependent on the incidence angle of the laser beam on the retina, which would be altered by an ERM.[15,16] Thus, the diagnostic value of examining the photoreceptor microstructures by SD-OCT in eyes with an ERM may not be as reliable as in cases of acute zonal occult outer retinopathy and other outer retinal diseases where the inner retinal alterations do not attenuate the laser energy.

The purpose of this study was to evaluate the relationship between deteriora-

Author Affiliations: Department of Ophthalmology, National Tokyo Medical Center (Drs Watanabe, Akiyama, and Noda), and Laboratory of Visual Physiology, National Institute of Sensory Organs (Drs Tsunoda and Mizuno), Tokyo, Japan.

tion of the best-corrected visual acuity (BCVA) and abnormalities of the photoreceptor microstructures in patients with untreated idiopathic ERM. To accomplish this, we examined cases with ERM without severely deformed inner structures, such as a lamellar hole and large cystic formations. We classified the abnormalities of the retina in the SD-OCT images and performed multiple regression analyses to determine which parameter was independently and significantly associated with the BCVA in cases of ERM.

## METHODS

This was a retrospective case series performed in the Department of Ophthalmology, National Tokyo Medical Center, Tokyo, Japan. After an explanation of the procedures to be used, an informed consent was received from all of the subjects for the tests. The procedures used adhered to the tenets of the Declaration of Helsinki, and approval to perform this study was obtained from the review board/ethics committee of the Tokyo Medical Center.

We examined 52 eyes of 45 patients (20 eyes of 18 men and 32 eyes of 27 women, mean [SD] age, 67.0 [10.0] years) diagnosed with an ERM without lamellar holes or apparent cystic changes in the fovea. The patients were examined between October 2009 and September 2010. The exclusion criteria were myopia more than 6 diopters, advanced lens opacification, other ocular disease that could cause visual disturbances, secondary ERM caused by vascular diseases, uveitis, and retinal detachment. Cases whose OCT images did not have enough signal intensity for evaluation, ie, average intensity of the SD-OCT signal was less than 8 of 10, were also excluded.

Spectral-domain OCT (Cirrus HD-OCT, versions 4.5 and 5.1; Carl Zeiss Meditec) was used to obtain tomographic images of the retina. Following dilation of the pupil, 5 line-scan images were obtained both horizontally (length, 9.0 mm) and vertically (length, 6.0 mm) across the foveola, with the distance between each scan line of 0.075 mm. Cases where any of the scan lines did not pass through the foveola were excluded.

Eight SD-OCT features were evaluated: (1) central retinal thickness (CRT), (2) COST line, (3) IS/OS junction line, (4) bulgelike appearance of the IS/OS junction line at the foveola (foveal bulge), (5) external limiting membrane (ELM), (6) internal limiting membrane (ILM), (7) foveal pit, and (8) ERM formation over the foveal center.

The CRT was defined as the distance between the inner retinal surface and inner surface of the retinal pigment epithelium at the foveola (**Figure 1**A). It was measured manually by the built-in scale of the SD-OCT system.

The microstructures within a 500-μm diameter of the fovea (Figure 1A, scale bar) were graded independently by 2 experienced ophthalmologists (K.W. and K.T.) (**Table 1**) to be either normal or abnormal. During this procedure, all the patients' information, including the BCVA, was masked to the examiners. In cases where the gradings were different, discussions were held until both examiners agreed. In earlier studies, the OCT features were graded into 3 classes, eg, normal ILM, mild ILM distortion, and severe ILM distortion.[7,9,17] We initially adopted a similar classification; however, we found it confusing especially in distinguishing mildly from severely abnormal structures. We have thus simplified the classification to normal or abnormal.

The COST line, IS/OS junction line, and ELM were graded normal when they were seen clearly and appeared continuous in the foveal region, and they were graded abnormal when they were blurred, interrupted, or absent. The foveal bulge is an elevation of the IS/OS junction line that appears like a dome over the foveola. We graded it normal when the bulgelike appearance was clearly observed and graded it abnormal when the bulgelike appearance was not observed and the IS/OS junction line appeared flat.

The ILM was graded normal when it looked smooth and flat at the fovea and was graded abnormal when it looked wrinkled or distorted. The foveal pit was graded normal when the concave retinal surface was clearly observed at the foveola and graded abnormal when the foveal surface appeared flat. The ERM was graded normal when the ERM did not overlap the foveola and graded abnormal when the ERM was attached over the foveola.

The relationship between these 8 OCT features and the visual acuity was statistically examined. Statistical analysis was performed using SPSS version 19.0 (SPSS Japan). The visual acuity was converted to logMAR units for the statistical analyses. Pearson correlations were performed to determine the association between CRT and visual acuity. The Mann-Whitney test was used to compare the BCVA and CRT between the normal and abnormal groups for each OCT feature. Multiple regression analysis was performed with BCVA and CRT as the dependent variables and with the integrities of 7 OCT features as independent variables. A $P$ value $<.05$ was considered significant.

## RESULTS

We first evaluated the normal fellow eyes of 29 of the 45 patients studied (13 eyes of 13 men and 16 eyes of 16 women; mean [SD] age, 66.0 [8.1] years). For these, all of the 7 OCT features were judged normal.[18]

Two representative cases demonstrating how the OCT features were judged to be either normal or abnormal are shown in Figure 1B and C. A horizontal SD-OCT scan image of the left retina of a 74-year-old man is shown in Figure 1B. The ELM, foveal bulge, IS/OS junction line, and COST line were clearly observed and judged to be normal. An ERM was present over the foveola, and this was judged to be abnormal. The foveal pit was concave and judged to be normal. The ILM was partially wrinkled at the foveola and judged abnormal.

A vertical SD-OCT scan image of the right retina of a 65-year-old woman is shown in Figure 1C. The IS/OS junction line and ELM were clearly observed and judged to be normal. The foveal bulge and COST line could not be seen at the fovea and were judged abnormal. The ILM was wrinkled in the parafoveal region; however, the foveal region within 500 μm of the foveola was spared and judged normal. The foveal pit was judged abnormal because the fovea was elevated by a tangential traction from the ERM and the foveal pit was flattened. An ERM covered the foveola and was judged abnormal.

The BCVA and CRT of the normal eyes were compared with those of the abnormal groups for each OCT feature of the 52 cases by Mann-Whitney test (**Figure 2**). The BCVA was significantly better in cases when 6 OCT features were judged to be normal: COST line, IS/OS junction line, foveal bulge, ELM, foveal pit, and ERM (Figure 2A). The CRT was significantly thinner in cases when 5 OCT features were judged to be normal: COST line, IS/OS junction line, foveal bulge, foveal pit, and ERM (Figure 2B).

Subsequently, multiple regression analyses were performed to determine the independent predictors of the BCVA and CRT in eyes with an ERM. The analyses showed

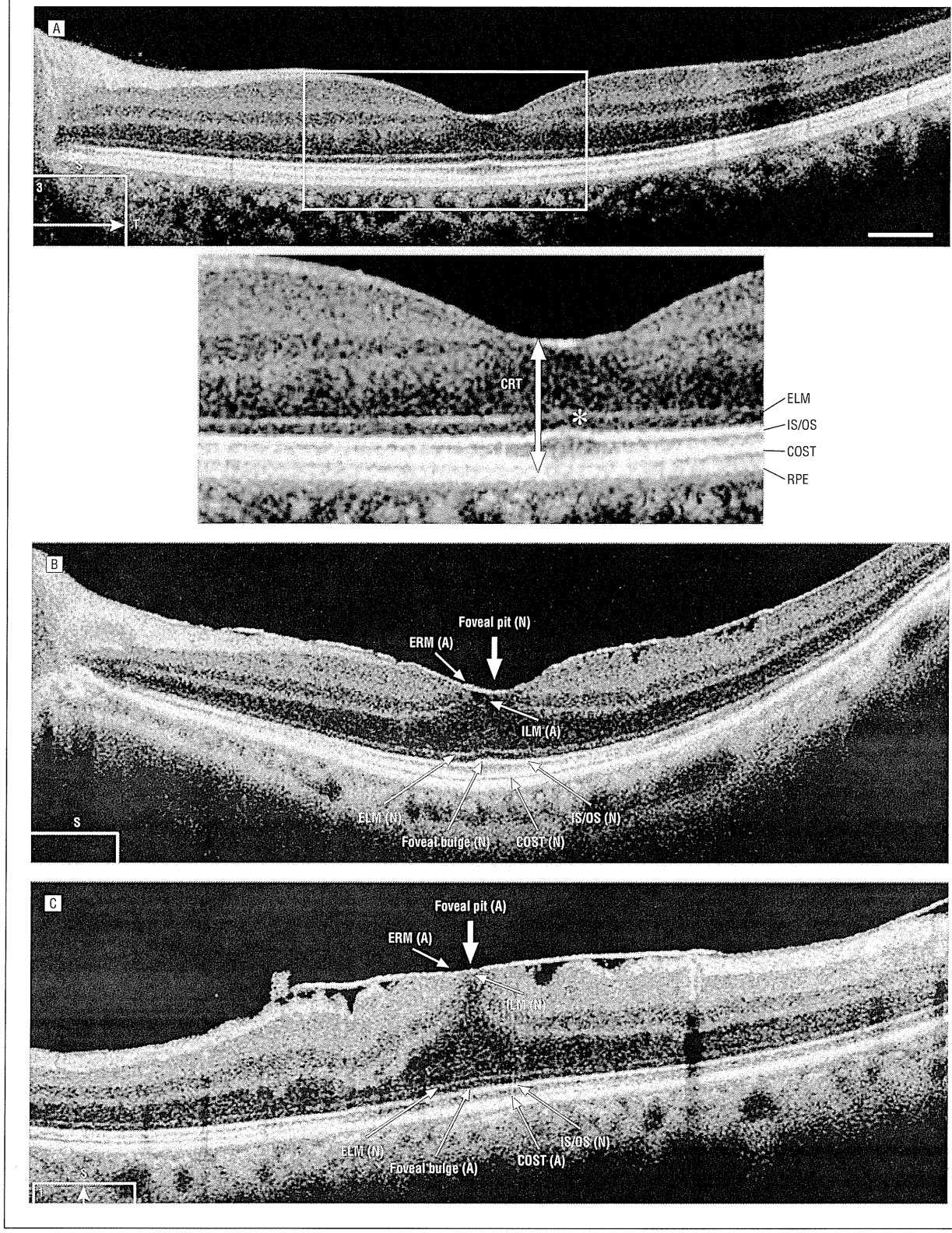


**Figure 1.** Optical coherence tomography images. A, Horizontal optical coherence tomography image of the retina of a normal eye with a magnified image showing the locations of the external limiting membrane (ELM), photoreceptor inner segment/outer segment junction line (IS/OS), cone outer segment tip line (COST), retinal pigment epithelium (RPE), foveal bulge (asterisk), and central retinal thickness (CRT) (arrow). Scale bar=500 µm. B and C, Classification of 7 features in spectral-domain optical coherence tomography image in patients with an epiretinal membrane (ERM). A indicates abnormal; ILM, internal limiting membrane; and N, normal.

**Table 1. Classification of OCT Features in the Foveal Region**

| Classification | COST | IS/OS | Foveal Bulge | ELM | ILM | Foveal Pit | ERM |
|---|---|---|---|---|---|---|---|
| Normal | Clear and continuous | Clear and continuous | Observed | Clear and continuous | Smooth and flat | Observed | Foveola is free of ERM |
| Abnormal | Blurred, interrupted, or absent | Blurred, interrupted, or absent | Not observed | Blurred, interrupted, or absent | Wrinkled or distorted | Not observed | ERM is attached over foveola |

Abbreviations: COST, cone outer segment tip line; ELM, external limiting membrane; ERM, epiretinal membrane; ILM, internal limiting membrane; IS/OS, photoreceptor inner segment/outer segment junction line; OCT, optical coherence tomography.

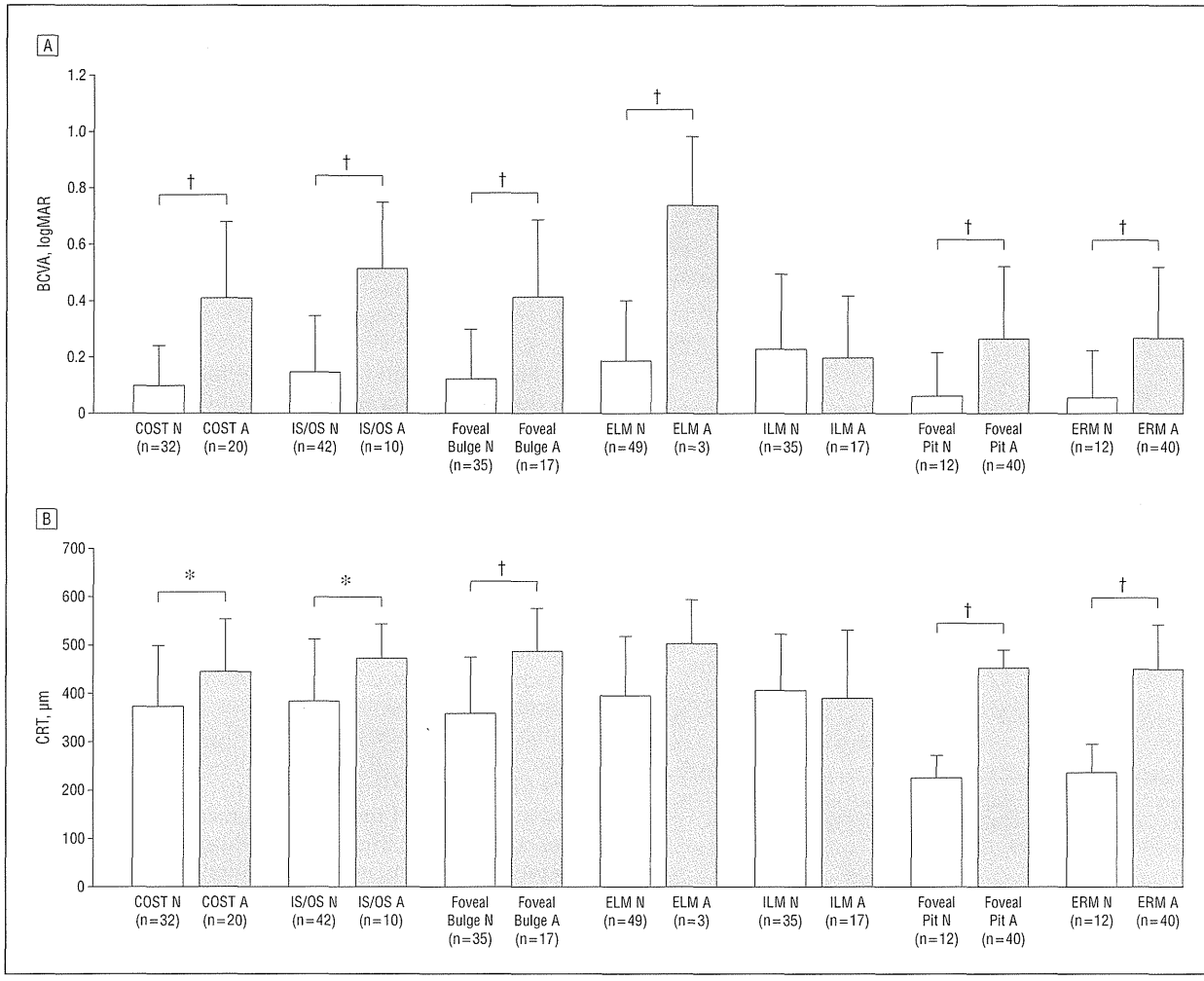


**Figure 2.** Comparisons between normal (N) and abnormal (A) eyes for 7 optical coherence tomography features. A, Best-corrected visual acuity (BCVA). B, Central retinal thickness (CRT). Mann-Whitney test, $*P < .05$ and $\dagger P < .01$. COST indicates cone outer segment tip line; ELM, external limiting membrane; ERM, epiretinal membrane; ILM, internal limiting membrane; and IS/OS, inner segment/outer segment junction line.

that the predictive variables for BCVA were COST line ($P < .001$), IS/OS junction line ($P = .02$), and ELM ($P = .03$). The standardized partial regression coefficient β was 0.415 for the COST line, 0.287 for the IS/OS junction line, and 0.247 for the ELM (**Table 2**). On the other hand, the predictive variables for the CRT were foveal pit ($P < .001$), ERM ($P = .003$), and foveal bulge ($P = .04$). The standardized partial regression coefficient β was 0.476 for the foveal pit, 0.337 for the ERM, and 0.182 for the foveal bulge (**Table 3**).

The CRT was measured at the foveal center in 52 cases, and a significantly positive correlation was observed between the CRT and the BCVA ($r^2 = 0.274$; $P < .01$) (**Figure 3**).

## COMMENT

The relationships between the outer retinal microstructures determined by SD-OCT and the BCVA have been reported previously for patients with ERM.[7-10] The de-

**Table 2. Multiple Regression Analyses to Determine the Independent Predictors of the Best-Corrected Visual Acuity**

| | Standardized Partial Regression Coefficient (β) | *P* Value |
|---|---|---|
| COST | 0.415 | <.001 |
| IS/OS | 0.287 | .02 |
| ELM | 0.247 | .03 |

Abbreviations: COST, cone outer segment tip line; ELM, external limiting membrane; IS/OS, photoreceptor inner segment/outer segment junction line.

**Table 3. Multiple Regression Analyses to Determine the Independent Predictors of the Central Retinal Thickness**

| | Standardized Partial Regression Coefficient (β) | *P* Value |
|---|---|---|
| Foveal pit | 0.476 | <.001 |
| ERM | 0.337 | .003 |
| Foveal bulge | 0.182 | .04 |

Abbreviation: ERM, epiretinal membrane.

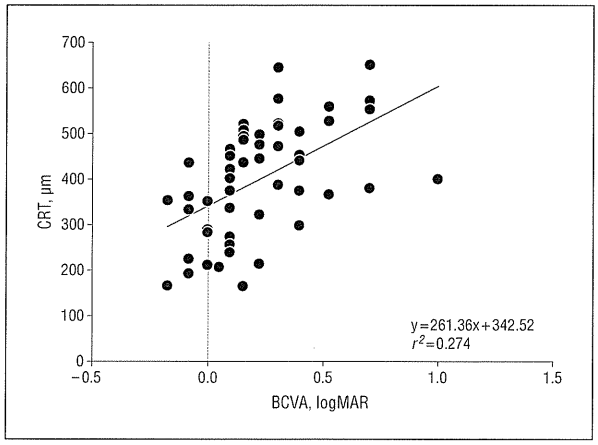


**Figure 3.** Significant correlation between central retinal thickness (CRT) and best-corrected visual acuity (BCVA) in 52 eyes. Pearson correlation coefficient $r^2$ was 0.274 ($P < .01$).

sign of our study was different from these earlier studies because we evaluated the OCT features only in the foveal region within 500 μm of the center because the visual acuity is mainly determined by the foveal center. In addition, we excluded patients who had small lamellar holes or apparent cystic changes in the fovea, which can induce optical artifacts and distort the appearances of the photoreceptor layer in the OCT images.

Multiple regression analyses showed that the integrity of the COST line was most strongly associated with the BCVA, followed by the IS/OS junction line and the ELM. On the other hand, the foveal bulge, ILM, foveal pit, and ERM were not significantly associated with the BCVA. It has been reported that the integrity of the IS/OS junction line is significantly associated with the postoperative BCVA.[7,8] Our results showed that not only the IS/OS junction but also the COST line were most strongly associated with the preoperative BCVA (β = 0.415 for COST line; β = 0.287 for IS/OS junction). Abnormalities of the COST line have been suggested to be an early sign of photoreceptor dysfunction in eyes with outer retinal disorders.[11,19] In cases of ERM, the appearance of the COST line at the fovea should be carefully examined to determine if early changes in retinal function might be present.

In patients with an ERM, the retinal thickening could affect the appearance of the images of the photoreceptor layer. Multiple regression analysis showed that abnormalities in the COST line, IS/OS junction line, and ELM were not significantly associated with the CRT (Table 2 and Table 3), although an absence of the foveal pit ($P < .001$) and existence of foveal ERM over the foveola ($P = .003$) were independently associated with the CRT. These results suggest that the photoreceptor microstructures appeared abnormal not because of the reduced laser light through thickened retina but because of real morphological changes. The abnormality in the inner retinal structures, eg, ILM, foveal pit, and ERM at the foveola, might affect the visual acuity because they would alter the optical characteristics of the retina. However, the results of multiple regression analysis showed that these inner retinal abnormalities did not significantly contribute to the BCVA at least in the early stage of ERM.

The correlations between the 4 highly refractive bands in the outer retina seen in the SD-OCT images and the retinal histologic features have been well investigated.[16,20,21] There has been an early consensus on the interpretation of the first and fourth bands in the outer retina, the innermost band representing the ELM and the outermost band representing the complex of the retinal pigment epithelium and Bruch membrane. The second band was initially thought to arise from the differences in the refractive index between the inner and outer segments of the photoreceptor and thus called the photoreceptor IS/OS junction line. However, Fernández et al[21] found it to represent the ellipsoids of the photoreceptor inner segment by ultra high-resolution OCT with adaptive optics. The third band has been found to represent the junction between the cone outer segment and the apical microvillae of the retinal pigment epithelium and is called the COST line.[16,21] The ellipsoids in the photoreceptor inner segments are rich in mitochondria and crucial for the metabolism of the photoreceptors. The cone outer segments contain the photopigment discs, which are also important for phototransduction. The strong contributions of the COST and IS/OS junction lines to the BCVA but not to the CRT suggest that both the microstructure and function of the photoreceptors were damaged by the ERM.

The OCT abnormalities in the photoreceptor microstructures have been reported to be significantly correlated with the loss of visual acuity and visual field in acute zonal occult outer retinopathy and retinal dystrophies where the photoreceptors are primarily affected.[11-14] On the other hand, the abnormal ERM develops on the surface of the retina without directly affecting the photoreceptor layer. The membrane can then cause tangential traction over the macula, followed by an inward traction toward the vitreous cavity at the foveal pit. Long-standing inward traction may cause formations of cysts in the outer nuclear layer

and microstructural changes in the photoreceptor.[7,8,22,23] Thus, the etiology of the OCT abnormalities of the photoreceptor layer observed in eyes with an ERM should be different from that of outer retinal diseases.

Niwa et al[24] measured focal macular electroretinograms (fmERGs) elicited by 15° stimuli in 37 patients with an ERM and concluded that the inner retinal layer was predominantly impaired initially and that the visual dysfunction in eyes with ERM may have resulted from macular edema. They also found that the correlation between the visual acuity and the degree of amplitude reduction of the a wave, b wave, and oscillatory potentials was not significant. However, they reported that the visual acuity largely depended on a very limited region of the fovea, and the stimulated region of 15° in the fmERG was too large to evaluate the relationship between the BCVA and fmERGs. In fact, there are patients with macular dystrophy who have both good visual acuity and extinguished fmERGs.[19] In such patients, the function of a very small region of the fovea is spared. In cases of ERM, an inward traction is especially strong in the foveola as shown in Figure 1B and C, and the outer nuclear layer within 500 μm of the foveola is thicker than in the parafoveal region. Thus, the results of fmERGs elicited by 15° stimuli did not necessarily exclude the fact that the photoreceptor function was primarily affected by the ERM. Considering that mechanical traction is extraordinarily severe in the foveola, the photoreceptor function may be primarily impaired even at the early stage of ERM, leading to the reduction of the BCVA.

There are reports that the reduction in the visual acuity in eyes with an ERM is due to retinal thickening,[9,10] and our results also indicated that the thickness of the outer retina, ie, combined thickness of outer nuclear layer and photoreceptor layer, was correlated with visual acuity (Figure 3). Together with the results of multiple regression analysis, functional damage of the photoreceptor due to long-standing inward traction was determined to be a strong contributor to the visual acuity reduction. Thus, detailed examinations of the photoreceptor microstructures in the OCT images may help find early visual dysfunction in cases of idiopathic ERM.

**Submitted for Publication:** July 4, 2012; accepted July 19, 2012.
**Correspondence:** Kazushige Tsunoda, MD, PhD, Laboratory of Visual Physiology, National Institute of Sensory Organs, 2-5-1 Higashigaoka, Meguro-ku, Tokyo 152-8902, Japan (tsunodakazushige@kankakuki.go.jp).
**Conflict of Interest Disclosures:** None reported.
**Funding/Support:** This research is supported in part by research grants from the Ministry of Health, Labor, and Welfare, Japan, and Grant-in-Aid for Scientific Research, Japan Society for the Promotion of Science.

## REFERENCES

1. Keane PA, Liakopoulos S, Chang KT, et al. Relationship between optical coherence tomography retinal parameters and visual acuity in neovascular age-related macular degeneration. *Ophthalmology.* 2008;115(12):2206-2214.
2. Piccolino FC, de la Longrais RR, Ravera G, et al. The foveal photoreceptor layer and visual acuity loss in central serous chorioretinopathy. *Am J Ophthalmol.* 2005;139(1):87-99.
3. Otani T, Yamaguchi Y, Kishi S. Correlation between visual acuity and foveal microstructural changes in diabetic macular edema. *Retina.* 2010;30(5):774-780.
4. Ota M, Tsujikawa A, Murakami T, et al. Foveal photoreceptor layer in eyes with persistent cystoid macular edema associated with branch retinal vein occlusion. *Am J Ophthalmol.* 2008;145(2):273-280.
5. Itoh Y, Inoue M, Rii T, Hiraoka T, Hirakata A. Significant correlation between visual acuity and recovery of foveal cone microstructures after macular hole surgery. *Am J Ophthalmol.* 2012;153(1):111-119, e1.
6. Wakabayashi T, Fujiwara M, Sakaguchi H, Kusaka S, Oshima Y. Foveal microstructure and visual acuity in surgically closed macular holes: spectral-domain optical coherence tomographic analysis. *Ophthalmology.* 2010;117(9):1815-1824.
7. Falkner-Radler CI, Glittenberg C, Hagen S, Benesch T, Binder S. Spectral-domain optical coherence tomography for monitoring epiretinal membrane surgery. *Ophthalmology.* 2010;117(4):798-805.
8. Suh MH, Seo JM, Park KH, Yu HG. Associations between macular findings by optical coherence tomography and visual outcomes after epiretinal membrane removal. *Am J Ophthalmol.* 2009;147(3):473-480, e3.
9. Michalewski J, Michalewska Z, Cisiecki S, Nawrocki J. Morphologically functional correlations of macular pathology connected with epiretinal membrane formation in spectral optical coherence tomography (SOCT). *Graefes Arch Clin Exp Ophthalmol.* 2007;245(11):1623-1631.
10. Arichika S, Hangai M, Yoshimura N. Correlation between thickening of the inner and outer retina and visual acuity in patients with epiretinal membrane. *Retina.* 2010;30(3):503-508.
11. Tsunoda K, Fujinami K, Miyake Y. Selective abnormality of cone outer segment tip line in acute zonal occult outer retinopathy as observed by spectral-domain optical coherence tomography. *Arch Ophthalmol.* 2011;129(8):1099-1101.
12. Sergouniotis PI, Holder GE, Robson AG, Michaelides M, Webster AR, Moore AT. High-resolution optical coherence tomography imaging in KCNV2 retinopathy. *Br J Ophthalmol.* 2012;96(2):213-217.
13. Genead MA, Fishman GA, Rha J, et al. Photoreceptor structure and function in patients with congenital achromatopsia. *Invest Ophthalmol Vis Sci.* 2011;52(10):7298-7308.
14. Hood DC, Zhang X, Ramachandran R, et al. The inner segment/outer segment border seen on optical coherence tomography is less intense in patients with diminished cone function. *Invest Ophthalmol Vis Sci.* 2011;52(13):9703-9709.
15. Lujan BJ, Roorda A, Knighton RW, Carroll J. Revealing Henle's fiber layer using spectral domain optical coherence tomography. *Invest Ophthalmol Vis Sci.* 2011;52(3):1486-1492.
16. Srinivasan VJ, Monson BK, Wojtkowski M, et al. Characterization of outer retinal morphology with high-speed, ultrahigh-resolution optical coherence tomography. *Invest Ophthalmol Vis Sci.* 2008;49(4):1571-1579.
17. Mitamura Y, Hirano K, Baba T, Yamamoto S. Correlation of visual recovery with presence of photoreceptor inner/outer segment junction in optical coherence images after epiretinal membrane surgery. *Br J Ophthalmol.* 2009;93(2):171-175.
18. Rii T, Itoh Y, Inoue M, Hirakata A. Foveal cone outer segment tips line and disruption artifacts in spectral-domain optical coherence tomographic images of normal eyes. *Am J Ophthalmol.* 2012;153(3):524-529, e1.
19. Tsunoda K, Usui T, Hatase T, et al. Clinical characteristics of occult macular dystrophy in family with mutation of RP1l1 gene. *Retina.* 2012;32(6):1135-1147.
20. Spaide RF, Curcio CA. Anatomical correlates to the bands seen in the outer retina by optical coherence tomography: literature review and model. *Retina.* 2011;31(8):1609-1619.
21. Fernández EJ, Hermann B, Povazay B, et al. Ultrahigh resolution optical coherence tomography and pancorrection for cellular imaging of the living human retina. *Opt Express.* 2008;16(15):11083-11094.
22. Wilkins JR, Puliafito CA, Hee MR, et al. Characterization of epiretinal membranes using optical coherence tomography. *Ophthalmology.* 1996;103(12):2142-2151.
23. Gaudric A. Macular cysts, holes and cavitations: 2006 Jules Gonin lecture of the Retina Research Foundation. *Graefes Arch Clin Exp Ophthalmol.* 2008;246(7):1071-1079.
24. Niwa T, Terasaki H, Kondo M, Piao CH, Suzuki T, Miyake Y. Function and morphology of macula before and after removal of idiopathic epiretinal membrane. *Invest Ophthalmol Vis Sci.* 2003;44(4):1652-1656.